bioRxiv preprint doi: https://doi.org/10.1101/234286; this version posted October 18, 2018. The copyright holder for this preprint (which was not certified by peer review) is the author/funder, who has granted bioRxiv a license to display the preprint in perpetuity. It is made available under aCC-BY-ND 4.0 International license.



# Bundle-sheath cells are leaf "water valves" controlled by an $H^+$-ATPase via xylem acidification

**One-sentence summary:**

Cells enwrapping the leaf veins control the leaf hydraulic conductance by xylem sap pH regulated by a proton-pump

Yael Grunwald*[1], Noa Wigoda*[1,3], Nir Sade[1,2], Adi Yaaran[1], Tanmayee Torne[1], Sanbon Chaka Gosa[1], Nava Moran[1] and Menachem Moshelion[1].

[1] The R.H. Smith Institute of Plant Sciences and Genetics in Agriculture, The R.H. Smith Faculty of Agriculture, Food and Environment, The Hebrew University of Jerusalem, Rehovot, 76100 Israel

[2] School of Plant Sciences and Food Security, The George S. Wise Faculty of Life Sciences at Tel-Aviv University, Tel Aviv 6997801, Israel.

[3] Life Sciences Core Facilities department, Weizmann Institute of Science, Rehovot 76100 Israel

* Both authors contributed equally to this work.

bioRxiv preprint doi: https://doi.org/10.1101/234286; this version posted October 18, 2018. The copyright holder for this preprint (which was not certified by peer review) is the author/funder, who has granted bioRxiv a license to display the preprint in perpetuity. It is made available under aCC-BY-ND 4.0 International license.



## Abstract

Bundle-sheath cells (BSCs), parenchymatous cells tightly enwrapping the leaf veins, constitute a selective and dynamic barrier to solutes and water. The over three-fold-higher abundance of the AHA2 (Arabidopsis $H^+$-ATPase2) transcript we recently reported in Arabidopsis BSCs (compared to mesophyll cells) suggests AHA2 participation in this barrier function. Manipulating AHA2 activity in BSCs pharmacologically and genetically, while monitoring the xylem sap pH by fluorescence imaging of FITC-dextran fed into veins of detached leaves, demonstrated AHA2 indispensability for low sap pH, resolving the decades-lasting controversy about the molecular *origin* of xylem sap acidification. Furthermore, both AHA2 activity and sap acidification by added buffers enhanced the hydraulic leaf conductance, while alkaline sap pH – buffered or in AHA2 knockouts – reduced it. Similarly, the osmotic water permeability of isolated BSC protoplasts was reduced by alkaline and enhanced by acidic pH, thereby revealing the cellular mechanism underlying the above causative link between AHA2 activity and leaf water influx. This positions the BSCs as a transpiration-controlling valve in series with the stomata.

## Introduction

The majority (95%) of nutrients and water which enter the plant through the roots move upward as bulk via xylem vessels (Taiz and Zeiger, 2014) all the way into the leaf veins. On its way out of the leaf xylem and into the leaf photosynthetic tissue, the mesophyll, this transpiration stream crosses a layer of parenchymatous cells (bundle sheath cells, BSCs) which tightly enwrap the entire vasculature (Kinsman and Pyke, 1998). BSCs have been shown to act as a selective barrier between the vein and the mesophyll, capable of impeding, for example, the transport of sodium (in the banana leaf (Shapira et al., 2009)) and of boron (in the leaves of Thelungiella (Lamdan et al., 2012), and of Arabidopsis (Shatil-Cohen and Moshelion, 2012), and of banana (Shapira et al., 2013)), as well as the passage of water (Shatil-Cohen et al., 2011; Pantin et al., 2013). However, it is still not clear (Geilfus, 2017) whether and how the apoplastic (xylem) milieu

bioRxiv preprint doi: https://doi.org/10.1101/234286; this version posted October 18, 2018. The copyright holder for this preprint (which was not certified by peer review) is the author/funder, who has granted bioRxiv a license to display the preprint in perpetuity. It is made available under aCC-BY-ND 4.0 International license.



modulates the "barrier behavior" of the bundle sheath, and in particular, whether this behavior depends on the xylem sap pH.

While under normal growth conditions the leaf apoplast pH is around 5.5-6 (reviewed by Grignon and Sentenac, 1991; Geilfus, 2017). The rare direct determinations of leaf xylem pH placed it at 6.3-6.7 in cotton leaves (Hartung et al., 1988), or at 5.3 in sunflower leaves (Jia and Davies, 2007). The leaf xylem sap pH can change in response to external conditions. For example, the leaf xylem sap alkalinized when tomato roots were exposed to drying soil or supplied with nitrate (Jia and Davies, 2007), or when detached sunflower leaves were supplied with $HCO_3^-$ (Mengel, 1994). In turn, changes in the leaf xylem sap pH regulate physiological processes. For example, feeding high-pH solutions to detached leaves reduced stomatal conductance and transpiration both in *Commelina communis* and in tomato (Wilkinson and Davies, 1997; Wilkinson et al., 1998; Jia and Davies, 2007). As changes in pH define the dissociation state of weak acids, among them the major phytohormones abscisic acid (ABA) and indol acetic acid (IAA, auxin), they would thereby affect both their distribution between the apoplast and the cellular compartments of the plant, and hence, their biological activities. This has been shown, for example, for ABA accumulation in the alkalinizing xylem sap of a gradually dehydrated detached cotton leaf, which could be prevented by a pretreatment with an $H^+$-ATPase-activating fungal toxin, fusicoccin (Hartung et al., 1988).

Moreover, xylem sap pH is likely a crucial component of the proton-motive force governing transmembrane transport between the xylem and the surrounding BSCs. Yet, in spite of its importance to the plant basic life processes, molecular evidence linking a specific $H^+$-ATPase to the pH regulation of the leaf xylem sap and to the ensuing physiological changes in the leaf is missing.

$H^+$-ATPases constitute a family of proton pumps driven by hydrolysis of ATP and are found in the plasma membrane of plants and fungi (Axelsen and Palmgren, 2001). 11 $H^+$-ATPases isoforms have been reported in Arabidopsis; among them, the AHA1 and AHA2 are by far the most abundantly expressed members of this family throughout plant

bioRxiv preprint doi: https://doi.org/10.1101/234286; this version posted October 18, 2018. The copyright holder for this preprint (which was not certified by peer review) is the author/funder, who has granted bioRxiv a license to display the preprint in perpetuity. It is made available under aCC-BY-ND 4.0 International license.



life and tissues (Haruta et al., 2010). The expression of a GUS reporter gene in Arabidopsis, under the *AHA2* promoter, revealed abundant expression specifically in roots and leaves, and especially in the vascular tissue (Fuglsang et al., 2007). Our transcriptome analysis of protoplasts isolated from Arabidopsis BSCs and mesophyll cells (MCs) showed that the BSCs express the *AHA2* gene at a threefold higher level than the MCs, while the *AHA1* gene expression, though abundant, was not different between these two cell types (Wigoda et al., 2017). Here we show that BSCs act as an active barrier between xylem and mesophyll: (a) it is mainly the activity of AHA2 of the BSCs which acidifies the sap, (b) the xylem sap pH regulates the radial hydraulic conductance of the leaf and (c) pH regulates the osmotic water permeability of the individual isolated BSCs protoplasts. We thus demonstrate a causative link between the activity of AHA2 and the hydraulic conductance of the leaf and reveal that its underlying mechanism is the pH-controlled osmotic water permeability of the BSCs.

## Results

### The effect of pharmacological agents – a pump stimulator and an inhibitor – on xylem pH

We used the fluorescence of FITC-dextran (10 kDa) perfused via petioles into detached WT Arabidopsis leaves to monitor the pH within the leaf minor veins (Materials and methods, Suppl. Figs S1-S2). When 10 µM fusicoccin (a fungal stimulator of P-type proton pumps, Serrano, 1988) was fed into the xylem, we observed a sharp decrease in xylem sap pH of about two pH units compared with leaves in control conditions (Figs. 1Ai, 1Aii, 1B) approximately 30 minutes after addition of fusicoccin. ETOH, the fusicoccin solvent, by itself, had no impact on xylem pH (Suppl. Fig. S3).

Further, WT leaves treated with 1 mM of vanadate (a commonly used P-type $H^+$-pump inhibitor (reviewed by Palmgren, 2001), in a high-$K^+$ solution (10 mM $KNO_3$), resulted in xylem sap alkalization of about one pH unit within 30-40 min (Figs. 1Aiii, 1Aiv, 1C).

bioRxiv preprint doi: https://doi.org/10.1101/234286; this version posted October 18, 2018. The copyright holder for this preprint (which was not certified by peer review) is the author/funder, who has granted bioRxiv a license to display the preprint in perpetuity. It is made available under aCC-BY-ND 4.0 International license.



Interestingly, neither a similar exposure to vanadate in the low-$K^+$ solution (XPS without added $KNO_3$, suppl. Fig.S4A), nor the high-$K^+$ solution by itself (Suppl. Fig. S4B) had any effect on the xylem sap pH.

**AHA2 acidifies the xylem pH**

In an attempt to resolve between the relative contributions of the two abundant $H^+$-ATPAses of the BSCs, AHA1 and AHA2 (Wigoda et al., 2017), to the acidification of the xylem pH, we compared the xylem sap pH of WT plants to that in T-DNA-insertion mutants of either pump. We used two independent mutant lines with a homozygous loss of function of the *AHA2* gene (*aha2-4* and *aha2-5*) and three such lines with mutated *AHA1* (*aha1-6, aha1-7, aha1-8*). The xylem sap pH of both *AHA2* mutants, *aha2-4* and *aha2-5*, was consistently higher, by 0.5-1 pH units, compared to the WT plants (Fig. 2A). In contrast, there was no significant difference between the xylem sap pH in WT vs. the three lines of AHA1 mutants (Suppl. Fig. S5).

To further test the ability of AHA2 to acidify the xylem sap pH, we complemented the *AHA2* deficient plants (the *aha2-4* mutant), with the *AHA2* gene directed specifically to the BSCs (under the BSCs-specific promotor Scarecrow, SCR; Wysocka-Diller et al., 2000). Using qRT-PCR on whole leaves of mature transgenic plants, we confirmed *AHA2* absence in the *aha2-4* mutant (Fig. 3A, as in Haruta et al., 2010), and demonstrated successful complementation in two lines (T55 and T56). The transcript level of *AHA2* in these lines was even higher than in the WT (Fig. 3A). While the xylem sap pH in the *AHA2*-knockout mutant, *aha2-4*, was significantly more alkaline than in WT plants (repeating the results of Fig. 2A above), upon the complementation of the *aha2-4* mutant with the BSC-directed *AHA2*, the xylem sap pH in both lines became no higher than WT (Fig 3B). The level of *AHA1* transcript in the whole leaf was not affected by the genetic manipulations of AHA2, neither by *AHA2* mutation (as in Haruta et al., 2010), nor by the BSC-specific mutant complementation with *AHA2* (Fig. S6).

**Basic pH lowers the leaf hydraulic conductance, $K_{leaf}$**

bioRxiv preprint doi: https://doi.org/10.1101/234286; this version posted October 18, 2018. The copyright holder for this preprint (which was not certified by peer review) is the author/funder, who has granted bioRxiv a license to display the preprint in perpetuity. It is made available under aCC-BY-ND 4.0 International license.



To examine the impact of AHA2 on the water economy of the whole leaf we determined the leaf water potential ($\Psi_{leaf}$) and its transpiration (E), and from these two we calculated the leaf hydraulic conductance ($K_{leaf}$, Eq. 1 in Materials and methods). We compared the $K_{leaf}$ in detached leaves of WT and of the *aha2-4* and *aha2-5* knockouts fed with unbuffered XPS. Notably, the $K_{leaf}$ of the mutants was appreciably lower than that of WT leaves, about 50 % in *aha2-4* and about 30 % in *aha2-5* (Fig. 4A) although all three leaf types transpired at a similar rate (Suppl. Figs. S7A and S7E). Furthermore, WT leaves perfused with $XPS^{b}$ buffered at pH 7.5 had $K_{leaf}$ lower by over 50% compared to WT leaves perfused with $XPS^{db}$ buffered at pH 6 (Fig. 4B), again, without a difference in their transpiration rate (Suppl. Figs. S7B and S7F).

### Basic pH lowers the osmotic water permeability coefficient of BSCs protoplast membrane, $P_f$

In order to test the hypothesis that the pH-dependent reduction in $K_{leaf}$ is due to a reduction in the water permeability of the BSCs membranes, we measured the osmotic water permeability coefficient, $P_f$, of BSC under two pH treatments, using GFP labeled BSCs, from SCR:GFP plants. The mean initial $P_f$ (see Materials and methods) of BSCs treated with pH 6 was ~8.5 fold higher than that of BSCs treated with pH 7.5. ($5.39 \pm 1$ μm sec $^{-1}$ and $0.63 \pm 0.2$ μm sec $^{-1}$, respectively, Fig. 5).

## Discussion

### The AHA2 of the BSCs is indispensable for the leaf xylem sap acidification

$H^{+}$-ATPases are well known regulators of the apoplastic pH which has a key role in cell ion homeostasis (Taiz and Zeiger, 2014). Here we demonstrate, for the first time, that AHA2 which resides in the BSCs plasma membrane, exerts a dominant role in the acidification of the xylem sap in leaves. This conclusion is based on four different complementing approaches used in our study.

bioRxiv preprint doi: https://doi.org/10.1101/234286; this version posted October 18, 2018. The copyright holder for this preprint (which was not certified by peer review) is the author/funder, who has granted bioRxiv a license to display the preprint in perpetuity. It is made available under aCC-BY-ND 4.0 International license.



(1) *In-vivo measurement of xylem pH*. The ratio of fluorescence intensity of FITC-dextran excited at two different wavelengths is independent of the absolute dye concentration and is related only to pH. By this dual excitation technique, any variations in dye concentration caused by dye loading, compartmentation, leakage and photo-bleaching can be compensated for, since with this dye these parameters have a similar effect on fluorescence intensities at both wavelengths. Hoffmann and Kosengarten (Hoffmann et al., 1992; Hoffmann and Kosegarten, 1995) successfully measured the apoplastic pH, pH gradient between various cell types in the apoplast of sunflower leaves, and changes of leaf apoplastic pH in response to the uptake of $NH_4^+$ and $NO_3^-$ via petioles. In maize, measurements using pH-sensitive microelectrodes validated FITC-dextran as a faithful reporter of apoplastic pH-conditions (Pitann et al., 2009). In using the membrane-impermeable FITC-Dextran fed to the Arabidopsis leaf via a petiole, we relied on earlier demonstrations of the tight isolation of the vascular system due to the bundle sheath (Kinsman and Pyke, 1998; Shatil-Cohen et al., 2011; Shatil-Cohen and Moshelion, 2012; Sade et al., 2014;). We were thus satisfied that the FITC probe remained confined and reported reliably on the pH from within the BSC-lined xylem apoplast of the minor veins (Fig. 1A).

(2) *The use of classical pharmacological agents*. An $H^+$-ATPase specific enhancer (fusicoccin) and inhibitor (vanadate), fed directly to the leaf xylem, established that pH acidification of the leaf xylem sap involves P-type proton pump(s) (AHAs), which extrude protons – most likely, from the BSCs – into the xylem lumen. Notably, in our experiments, vanadate increased the xylem sap pH only when it was administered in high-$K^+$ XPS, while vanadate in low-$K^+$ XPS did not cause any detectable pH change. We explain this requirement for 10 mM $KNO_3$ to show vanadate inhibition of the $H^+$-pump, as resulting from an increased concentration of substrate (the added $K^+$ and $NO_3^-$ ions) which can participate in secondary $H^+$-co-transport into the BSCs, thereby dissipating the protons from the xylem lumen. This conforms with the aforementioned general notion that the pH of an apoplastic compartment reflects, among others, a balance in bi-directional proton movements (Serrano, 1988). That proton-coupled $K^+$

bioRxiv preprint doi: https://doi.org/10.1101/234286; this version posted October 18, 2018. The copyright holder for this preprint (which was not certified by peer review) is the author/funder, who has granted bioRxiv a license to display the preprint in perpetuity. It is made available under aCC-BY-ND 4.0 International license.



transmembrane co-transport plays a particularly important role in the BSCs is suggested by the 10% higher expression in BSCs (relative to mesophyll cells) of two $K^+$ uptake permeases, AtKT2 and AtKUP11 (likely to be $H^+$-coupled (Wigoda et al., 2017) and references therein).

(3) *Genetic manipulation – knockouts.* We have established here, for the first time, the dominant role of AHA2 in regulating the xylem sap pH in Arabidopsis leaf. While the pH of xylem sap in both AHA2 mutant lines, a*ha2-4* and *aha2-5* was consistently higher than WT, xylem sap in the *aha1* mutant lines was no different than in WT.

(4) *Genetic manipulation – knockout complementation.* The xylem sap pH was restored to WT-like levels in two lines resulting from *aha2-4* complementation with the *AHA2* gene directed specifically into the BSCs, using the specific promotor SCR. Somewhat surprisingly, although the complementation was directed to BSCs, the AHA2 transcript levels in the whole leaf of the complemented plants were considerably higher than in the WT leaf. Nevertheless, the level of AHA2 activity – as reflected in the xylem sap pH (especially in the complemented line T55, where pH was intermediate between the mutant *aha2-4* and the WT) – was somewhat lower than could be expected from the transcript level. This may suggest a post-transcriptional regulation of the AHA2 in BSCs.

Moreover, we noticed a lack of a change in the transcript level of AHA1, not only in the mutant aha2-4, as already noted by Haruta et al., (2010), but also in the BSC-directed complementation lines T55 and T56 (Fig. S6). This lack of *inverted* correlation between the transcript levels of AHA1 and AHA2 in the above examples, contrary to what might be expected had they shared responsibility for the same function and, therefore would have been linked by a mutual feedback, is another indication for the already inferred relative specificity of AHA2 for its BSCs related function – the maintenance of xylem sap pH.

bioRxiv preprint doi: https://doi.org/10.1101/234286; this version posted October 18, 2018. The copyright holder for this preprint (which was not certified by peer review) is the author/funder, who has granted bioRxiv a license to display the preprint in perpetuity. It is made available under aCC-BY-ND 4.0 International license.



**The physiological relevance of extracellular pH**

*External alkalization reduces the osmotic water permeability ($P_f$) of the BSCs.* It had been established that low cytosolic pH inhibits aquaporin gating and in doing so reduces $P_f$ (Tournaire-Roux et al., 2003; Alleva et al., 2006). This phenomenon has been studied in roots under stress conditions such as flooding or drought, where a change in the water hydraulic permeability of the roots is considered to be part of the plant stress defense mechanism. External medium acidification also reduced $P_f$ in "right-side-out" red beet root PM vesicles (i.e., vesicles with aquaporin membrane topology the same as in the cell), which, because of a reduction of the activation energy for water transport was attributed to aquaporins (Alleva et al., 2006). In contrast, the fungal aquaporin RdAQP1, when expressed in Arabidopsis protoplasts, *elevated* the cell membrane water permeability at acidic external pH, but increasing the external pH to 7 abolished this elevation (Turgeman et al., 2016). The reduction in the fungal aquaporin activity with rising external pH was mediated by histidines facing the outside of the cell (*ibid.*). Here we demonstrate, for the first time in any plant cell, a reduction in $P_f$ driven by external alkalinization in a leaf bundle sheath cell, the BSC. Future work is required to clarify whether this $P_f$ reduction in BSCs is mediated by aquaporins and their external histidines.

*AHA2 role in the regulation of the whole leaf water balance.* The notion that AHA pumps, in general, power secondary $H^+$-cotransport across cell membranes facing the apoplast is decades old (Serrano, 1988; Sze et al., 1999; Palmgren, 2001). The plant plasma membrane $H^+$-ATPase has since been recognized as essential for plant growth (reviewed by Falhof et al., 2016). The practically sole "celebrated product" of its action to date is the proton motive force (PMF) – a gradient of protons concentration without- or in combination with an electrical gradient – which drives the movement of solutes across cellular membranes. In only a few cases has a *specific* physiological role been assigned to the plasma membrane $H^+$-ATPase – mainly in stomatal physiology and in roots (reviewed by Falhof et al., 2016). Here we show for the first time another, novel aspect of transport activity *regulated* (rather than *driven*) by AHA2 – that of water fluxes

bioRxiv preprint doi: https://doi.org/10.1101/234286; this version posted October 18, 2018. The copyright holder for this preprint (which was not certified by peer review) is the author/funder, who has granted bioRxiv a license to display the preprint in perpetuity. It is made available under aCC-BY-ND 4.0 International license.



from the xylem into the leaf and across the bundle sheath layer – evident as the leaf hydraulic conductance, $K_{leaf}$. We demonstrate a causative inverse correlation between the resulting $K_{leaf}$ and the xylem sap pH, be it pH manipulated directly by buffers, or altered genetically by abolishing AHA2 activity (in *AHA2* knockouts).

In an earlier work, Shatil-Cohen et al. (Shatil-Cohen et al., 2011) localized $K_{leaf}$ to the BSCs layer by showing that $K_{leaf}$ decreased when the BSCs were brought into direct contact with the plant stress hormone, abscisic acid (ABA) fed to the detached leaf, and not when ABA was smeared on the leaf surface. Our current work outlines a mechanism for this phenomenon: stress-induced xylem alkalization (already reported by others (Jia and Davies, 2007; Wang et al., 2012; Korovetska et al., 2014), likely due to ABA inhibition of the BSCs AHA2, similar to the $H^+$-ATPase inhibition seen in guard cells (Goh et al., 1996; Schroeder et al., 2001; Zhang et al., 2004), reduces the water permeability of the BSCs membranes. Consequently, the water permeability of the entire bundle sheath layer declines, demonstrating that under stress conditions it is an active hydraulic barrier. Here we show directly, using individual isolated BSCs, that $P_f$, the measure of the rate of water passage via the BSCs membranes, declines with external medium alkalinization. Such a pH rise could mediate the effect of ABA on BSCs in the detached leaf.

The results of this study broaden our basic understanding of how a leaf controls its water influx. Our results also support the notion that xylem sap alkalinization mediates the decline in plant shoot nutrient uptake due to abiotic stress. Here we focus specifically on the stress-induced cessation of activity of AHA2 in the BSCs, where we found the AHA2 instrumental in generating the low pH in the leaf xylem sap. The consequence of this decline of AHA2 activity and xylem sap alkalinization, is a decline in the PMF. Since AHA2 – via the PMF – powers the secondary, proton-coupled export and import of solutes across the BSCs membranes, not only does it regulate plant nutrition, but, very likely also drives the extrusion of toxic compounds from the xylem-lining cells into the

bioRxiv preprint doi: https://doi.org/10.1101/234286; this version posted October 18, 2018. The copyright holder for this preprint (which was not certified by peer review) is the author/funder, who has granted bioRxiv a license to display the preprint in perpetuity. It is made available under aCC-BY-ND 4.0 International license.



xylem, hence governing also the plant toxicity tolerance. These hypotheses await future experimentation.

In conclusion, rapid growth rate and high yields of crop plants are positively correlated with enhanced transpiration and $K_{leaf}$. Our finding that AHA2 regulates $K_{leaf}$ via xylem sap pH provides a molecular basis for understanding a novel aspect, other than just PMF, of the control that the xylem sap pH can exert in the leaf. This control, in combination with effects of PMF, is likely to underlie the plant's key physiological activities. These results provide a new focus for exploration and understanding the role of the involvement of BSCs in determining the xylem sap composition, and, in particular, their role as a transpiration-controlling valve in series with the stomata. BSCs are likely to become a key target tissue for the development of a new generation of manipulations for plant adaptation to environmental challenges.

bioRxiv preprint doi: https://doi.org/10.1101/234286; this version posted October 18, 2018. The copyright holder for this preprint (which was not certified by peer review) is the author/funder, who has granted bioRxiv a license to display the preprint in perpetuity. It is made available under aCC-BY-ND 4.0 International license.



## Materials and Methods

### Plant material

*Plant types*. We used WT (wild type) *Arabidopsis thaliana* plants ecotype Colombia, Col-0 (aka Col) and T-DNA insertion *AHA* mutants (Col) , *AHA1* mutants: *aha1-6 (*SALK_ 016325), *aha1-7 (*SALK_ 065288) and *aha1-8* (SALK_ 118350), and *AHA2* mutants; *aha2-4* (SALK_ 082786) and *aha2-5* (SALK_022010) obtained from the Arabidopsis Biological Resource Center (Ohio State University). The plants' genotypes were determined by PCR with allele-specific primers and then the single-gene knockout were confirmed for the absence of *AHA2 (or AHA1)* RNA using real time PCR (RT-PCR). The sequences of the PCR primers are provided in the supplemental Table S1. For the experiments of Fig. 5, we used SCR:GFP (Col) Arabidopsis plants expressing GFP specifically in the BSCs ER generated in our lab and described in detail by Attia et al., (2018)

*Plant Growth Conditions.* All plants were grown in soil as described by (Shatil-Cohen et al., 2011). Plants were kept in a growth chamber under short-day conditions (10-h light) and a controlled temperature of 20–22°C, with 70% humidity. Light intensity at the plant level of 100-150 μmol $m^{-2}$ $sec^{-1}$, using either fluorescent lights (Osram cool white, T5 FH 35W/840 HE, Germany) or LED light (EnerLED 24V-5630, 24W/m, 3000K (50%)/6000K(50%)). The plants were irrigated twice a week.

### Determination of xylem sap pH in detached leaves

*Leaf perfusion.* Leaves from 6-7 week old plants, approximately 2.5 cm long and 1 cm wide, were excised at the petiole base using a sharp blade and immediately dipped in "xylem perfusion solution" (XPS, see Solutions below), in 0.5 ml Eppendorf tubes for 30 minutes. Perfusion experiments using Safranin O (Sigma cat. #: S2255; 1% w/v in XPS) demonstrated that 30 minutes incubation sufficed for the whole leaf perfusion via the petiole by means of the transpiration stream (Fig. S1). All experiments were conducted between 1-4 hours from lights on.

bioRxiv preprint doi: https://doi.org/10.1101/234286; this version posted October 18, 2018. The copyright holder for this preprint (which was not certified by peer review) is the author/funder, who has granted bioRxiv a license to display the preprint in perpetuity. It is made available under aCC-BY-ND 4.0 International license.



The leaf xylem pH was determined using the dual-excitation membrane-impermeant fluorescent dye fluorescein isothiocyanate conjugated to 10 kD dextran (FITC-D; (Hoffmann and Kosegarten, 1995; Mühling et al., 1995)) dissolved in the solution perfused into the detached leaf. An *in-vivo* pH calibration curve was constructed using XPS buffered to predefined pH values (5, 5.5,6, 6.5, 7 and 7.5; see Solutions below). Effects of vanadate in high-$K^+$ solution or of fusicoccin in low-$K^+$ solution (i.e., in XPS) was tested in the absence of pH buffers (see Solutions below).

*Sample preparation on the microscope stage.* Immediately after the leaf xylem perfusion, the leaf was washed with that leaf's intended perfusate (the specific XPS to be tested) without the dye, laid on a microscope slide abaxial side up, and a drop of XPS (without the dye) was placed on top. Then, a thin layer of silicone high vacuum grease (Merck cat. #: 1.07921.0100) was applied around the leaf edge and a large coverslip (50 by 20 mm, larger than the leaf) was placed on the leaf and affixed to the slide beneath. The minor veins on the abaxial side were imaged via the coverslip.

*Fluorescence microscopy* was performed using an inverted microscope (Olympus-IX8 integrated within the Cell-R system, http://www.olympus-global.com), via an UPlanSApo 10*X*/0.40 (∞ /0.17/ FN26.5) objective. Pairs of images were recorded at a quick succession (at an approx. 200 ms interval) at two excitation wavelengths of 488 nm and 450 nm, and fluorescence at a single emission wavelength of 520 nm (Hoffmann and Kosegarten, 1995; Mühling et al., 1995) was recorded with a 12-bit CCD camera, Orca-AG (Hamamatsu, http:// www.hamamatsu.com) and saved in a linear 16 bit tiff format.

In all fluorescence microscopy experiments, each treatment was performed on at least five leaves, each from a different plant, on three days (all together, five biological repetitions in three independent experiments per treatment), alternating randomly among different treatments. Four to six paired images of a minor vein were obtained from different areas of each leaf (four-six technical repetitions per a biological repeat). For background values, leaves were perfused with experimental solutions without the dye; one leaf was sampled per treatment or plant type on each day of an experiment (all

bioRxiv preprint doi: https://doi.org/10.1101/234286; this version posted October 18, 2018. The copyright holder for this preprint (which was not certified by peer review) is the author/funder, who has granted bioRxiv a license to display the preprint in perpetuity. It is made available under aCC-BY-ND 4.0 International license.



together, at least three biological repetitions per treatment or plant type, a total of 20 leaves, with three technical repetitions per each biological repeat).

*Image analysis*. The acquired pairs of images were exported in a linear 16-bit tiff format for further processing with ImageJ (ver. 1.49V; http://rsbweb.nih.gov/ij/). The pixel by pixel ratio of the two images in each pair was calculated using the ImageJ 'Ratio-plus' plugin (Paulo J. Magalhães, 2004). The ratio calculation took into account the average background fluorescence at the corresponding excitation wavelength, which was subtracted from each pixel's fluorescence. Further analysis was performed on selected pixels, based on the image resulting from excitation at 488 nm. Only pixels with fluorescence values below the camera saturation level (<4095) and, at the same time, of at least 3 fold higher than the mean background value were selected (areas enclosed within yellow lines in the supplemental Fig. S2C). For each leaf (biological repeat), the mean fluorescence ratio obtained from a vein segment was converted to a pH value, using an *in-vivo* calibration curve, which was obtained, as described above, from paired images of WT leaves fed with pH-calibration solutions (see Solutions below). We occasionally verified the system stability using an *in-vitro* calibration curve, derived from imaging drops of the calibration solutions placed on microscope slides rather than fed into leaf veins. Also, changing the composition of the buffers (MES and HEPES) in the XPS had no effect on the calibration curve.

**Physiological characterization of the leaf (gas exchange and hydraulic conductance, $K_{leaf}$)**

*Sample preparation*. For Fig. 4A (and Suppl Figs. S7A, 7C, 7E), the leaves were excised in the evening preceding the measurements, in the light, shortly before the "lights OFF" transition, their petioles were dipped in the unbufferred High-$K^+$ XPS and placed in gas-sealed transparent 25 x 25 x 15 cm plastic boxes with water-soaked tissue paper on the bottom to provide ~100% humidity. Each leaves-containing box was then placed in another, lightproof box for the duration of the night. Measurements were conducted in the morning, between 10:00 AM and 12:00 PM, after 20 min illumination in the growth chamber.

bioRxiv preprint doi: https://doi.org/10.1101/234286; this version posted October 18, 2018. The copyright holder for this preprint (which was not certified by peer review) is the author/funder, who has granted bioRxiv a license to display the preprint in perpetuity. It is made available under aCC-BY-ND 4.0 International license.



For Fig. 4B (and Suppl. Figs. S7B, S7D, S7F), leaves were excised on the morning of the experiment, in the dark, about 10 min before the regular "lights ON" transition and their petioles were dipped in vials with buffered XPSdb (at pH, 6 and 7.5; see Solutions below). The vials were placed in gas-sealed transparent plastic boxes as described above. The boxes were then kept for two hours in the growth room under the regular light and temperature conditions. Prior to the measurements, the boxes were opened for 3 minutes to equilibrate with the ambient vapor pressure deficit (VPD) of 1.3-1.5 kPa. The measurements were conducted between 10:00AM and 1:00 PM (1-4 hours after lights ON).

*Gas-exchange assays, i.e.,* $g_s$ (stomatal conductance) and E (transpiration) were performed (as in Sade et al., 2014) using a Li-Cor 6400 portable gas-exchange system (LI-COR, USA https://www.licor.com/) equipped with a standard leaf cuvette with an aperture of 2 x 3 cm). The transfer time from box to Licor was at most 5 s. The measuring conditions were set to be as similar as possible to the growth chamber conditions (illumination: 150 µmol $m^{-2}$ $s^{-1}$; the amount of blue light was set to 10% of the photosynthetically active photon flux density to optimize stomatal aperture, the leaf temperature: approximately 24 °C, the VPD: approximately 1.3 kPa, and [$CO_2$] surrounding the leaf: 400 µmol $mol^{-1}$).

*Measuring the leaf water potential,* $\Psi_{leaf}$. Immediately following the gas exchange measurement which took about 5 min, the leaf was transferred to a pressure chamber (ARIMAD-3000; MRC Israel) equipped with a home-made silicon adaptor especially designed to fit Arabidopsis petioles into the chamber's O-ring. $\Psi_{leaf}$ was determined as described in (Sade et al., 2014).

*Determination of the leaf hydraulic conductance,* $K_{leaf}$. $K_{leaf}$ was calculated for each individual leaf as follows (Martre et al., 2000):

*Eq. 1:* $$K_{leaf} = E / (\Psi_{Leaf} - \Psi_{XPS}) \approx E / \Psi_{Leaf},$$

where E is the whole-leaf's transpiration, i.e., the water flux, and $\Psi_{Leaf}$ is the leaf water potential and $\Psi_{XPS}$ is the water potential of XPS (or of the $XPS^{db}$); as $\Psi_{XPS}$ is nearly null, in this calculaton we used solely the leaf water potential value.

bioRxiv preprint doi: https://doi.org/10.1101/234286; this version posted October 18, 2018. The copyright holder for this preprint (which was not certified by peer review) is the author/funder, who has granted bioRxiv a license to display the preprint in perpetuity. It is made available under aCC-BY-ND 4.0 International license.



**Protoplast isolation**

*For protoplast isolation,* Protoplasts were isolated from 6- to 8-week-old plants using the rapid method (Shatil-Cohen et al., 2014) with our pH 6 isotonic solution in the extraction procces (600 mOsmol, see solutions bellow).

**Osmotic water permeability coefficient ($P_f$) measurements**

$P_f$ was determined as described by Shatil-Cohen et al. (2014), except here we used an inverted epifluorescent microscope (Nikon eclipse TS100) with a 20x/NA 0.40 objective (Nikon) and a CCD 12 bit camera Manta G-235B (https://www.alliedvision.com), and an image-processing software AcquireControl® v5.0.0 (https://www.alliedvision.com). We recorded the BSCs swelling in response to hypo-osmotic challenge (of 0.37 MPa) generated by changing the bath solutions from an isotonic one (600 mOsm) to a hypotonic one (450 mOsm, *ibid.*). The challenges were performed at pH 6 and at pH 7.5. The osmolarity of these solutions (variants of the $XPS^{db}$; see Solutions) was adjusted with the appropriate amounts of D-sorbitol and was verified within 1% of the target value using a vapour pressure osmometer (Wescor). $P_f$ was determined from the initial rate of the cell volume increase using a numerical approach, in an offline curve-fitting procedure of the $P_f$Fit program, as described in Shatil-Cohen et al., (2014) and detailed in Moshelion et al., (2004). We present here the values of the intital $P_f$ ($P_{f_i}$) obtained by fitting model 5 (*ibid.*).

**Solutions**

*FITC-D dye* (Sigma cat. #: FD10S) was added from a 10 mM stock in water (kept aliquoted, protected from light, at -20 $^{o}$C) to all the XPS solutions (except in the autofluorescence assays) to a final conc. of 100 µM.

*XPS, basal Xylem Perfusion Solution*: 1 mM KCl, 0.3 mM $CaCl_2$ and 20 mM D-sorbitol (Sigma cat# 8143). Upon preparation, when unbuffered, the pH of this solution was 5.6 - 5.8 and its osmolarity was approx. 23 mOsm/L.

*Low-$K^+$ XPS:* the same as XPS above.

bioRxiv preprint doi: https://doi.org/10.1101/234286; this version posted October 18, 2018. The copyright holder for this preprint (which was not certified by peer review) is the author/funder, who has granted bioRxiv a license to display the preprint in perpetuity. It is made available under aCC-BY-ND 4.0 International license.



*High-$K^+$ XPS:* XPS + 10 mM $KNO_3$ and D-sorbitol adjustment to approx. 23 mOsm/L. Upon preparation, when unbuffered, the pH of this solution was 5.6 -5.8.

*$XPS^b$ (pH calibration solutions):* XPS buffered with 20 mM MES and HCl or NMG to pH 5, 5.5, or 6), or with 20 mM HEPES and NMG to pH 6.5, 7, or 7.5. Osmolarity of these solutions was adjusted with D-sorbitol to 23 mOsm/L.

*$XPS^{db}$*: High-$K^+$ XPS buffered with 10 mM MES and 10 mM HEPES and adjusted to pH 6 or 7.5 with N-Methyl D-glucamine (NMG). These solutions were adjusted with D-sorbitol to a final osmolarity of 40 mOsm/L.

*Solutions for leaf physiological characterization:* Non-buffered High-$K^+$ XPS (as above) was used for Figure 4A (and Suppl. Figs. S7A,S7C, S7E). $XPS^{db}$ was used for Fig. 4B (and Suppl. Figs. S7B, S7D, S7F).

*Solutions for $P_f$ determination:* pH 6 solutions : $XPS^{db}$ adjusted to pH 6 by NMG, and adjusted with D-sorbitol to either 450 mOsmol (hypotonic) or 600 mOsmol (isotonic); pH 7.5 solutions: $XPS^{db}$ adjusted to pH 7.5 by NMG, and adjusted with D-sorbitol to either 450 mOsmol (hypotonic) or 600 mOsmol (isotonic).

*Solution for protoplasts isolation:* pH 6 isotonic solution as for $P_f$ determination.

**Generation of SCR:AHA2-complemented plants**

*Vector construction*: *AHA2* gene was cloned into pDONR™ 221 (Invitrogene) vector and the SCR promoter into pDONRP4P1r using Gateway® compatible by BP reactions, and later cloned into the pB7M24GW (Invitrogene) two fragment binary vector by LR reaction according to the manufacturer's instructions. The binary *SCR:AHA2* vector was transformed into Agrobacterium by electroporation; transformants were selected on LB plates containing 25 µg/mL gentamycin and 50 µg/mL spectinomycin.

*aha2-4 and aha2-5 mutant lines transformation* with *SCR:AHA2:* was performed using the floral dip method (Clough and Bent, 1998). Transformants were selected based on their BASTA resistance, grown on plates with MS (Murashige and Skoog, Duchefa cat# M222.0050) Basal medium + 1 % sucrose and 20 µg/ml BASTA (Glufosinate Ammonium, Sigma cat # 45520). DNA insertion was verified in selected lines by PCR targeting the junction of *AHA2* and the 35S terminator with forward primer about 1000bp

bioRxiv preprint doi: https://doi.org/10.1101/234286; this version posted October 18, 2018. The copyright holder for this preprint (which was not certified by peer review) is the author/funder, who has granted bioRxiv a license to display the preprint in perpetuity. It is made available under aCC-BY-ND 4.0 International license.



from the 3' end of AHA2 and reverse primer on the 35S terminator (see primer list in supplemental Table S1).

**AHA2 gene expression in the whole leaf by qRT-PCR**

*RNA extraction and quantitative real-time (qRT-) PCR.* Total RNA was extracted from leaves using Tri-Reagent (Molecular Research Center, cat. #: TR 118) and treated with RNase-free DNase (Thermo Scientific™, cat. #: EN0525). Complementary DNA (cDNA) was prepared using the EZ-First Strand cDNA synthesis kit (Biological Industries cat. #: 2080050) according to the manufacturer's instructions. qRT-PCR was performed using C1000 Thermal Cycler (Bio-Rad), in the presence of EvaGreen (BIO-RAD cat.# 172-5204) and PCR primers to amplify specific regions of the genome (Haruta et al., 2010; suppl. Table S1). The results were analyzed using Bio Rad CFX manager™ software. Dissociation curve analysis was performed at the end of each qRT-PCR reaction to validate the presence of a single reaction product and lack of primer dimerization. Expression levels of examined genes were normalized using two normalizing genes (AT5G12240 and AT2G07734, Wigoda et al., 2017).

**Statistics**

The Student's unpaired two-tailed t-test was used for comparison of two means, which were considered to be significantly different at $P < 0.05$. For comparisons of three or more population means we used ANOVA, all-pairs Tuckey HSD (JMP® Pro 13), wherein different letters represent statistical differences at $P<0.05$. Images which yielded extreme ratio values which were more than 2.5 SD above the mean were discarded.

## Acknowledgments

We thank Ms. Dvorah Weisman of the Hebrew University of Jerusalem for help with image analysis and Dr. Shifra Ben-Dor of the Weizmann Institute of Science for comments on the manuscript.

bioRxiv preprint doi: https://doi.org/10.1101/234286; this version posted October 18, 2018. The copyright holder for this preprint (which was not certified by peer review) is the author/funder, who has granted bioRxiv a license to display the preprint in perpetuity. It is made available under aCC-BY-ND 4.0 International license.



This research was supported by the Israel Science Foundations, ISF (grants No.1312/12, and 1842/13 to NM, grant No. 878/16 to MM and a grant No. 12-01-0007 from the Israeli Chief Scientist, Ministry of Agriculture & Rural Development to MM and NM).

## Author Contributions

**Author contributions:**

N. Wigoda and Y. Grunwald planned performed and analyzed the experiments, and wrote the paper. A. Yaaran and T. Torne participated in generating the complemented plant lines, and A. Yaaran and S. Gosa participated in the leaf hydraulics determinations. N. Sade participated in the genotyping of the mutant AHA lines. M. Moshelion and N. Moran conceived the experiments, guided the students and wrote the paper.

## Competing interests

All authors declare they have no competing interests.

## Supplementary Materials

Figure S1. Perfusion of detached leaves via petioles

Figure S2. Image analysis details

Figure S3. Fusicoccin (and not its solvent EtOH by itself) lowered the leaf xylem sap pH

Figure S4. Neither vanadate in the *low-*$K^+$ XPS nor the high-$K^+$ XPS *without* vanadate affect the xylem sap pH in WT Arabidopsis

Figure S5. Knockout of AHA1 does not increase xylem sap pH in minor leaf veins of Arabidopsis leaf.

bioRxiv preprint doi: https://doi.org/10.1101/234286; this version posted October 18, 2018. The copyright holder for this preprint (which was not certified by peer review) is the author/funder, who has granted bioRxiv a license to display the preprint in perpetuity. It is made available under aCC-BY-ND 4.0 International license.



Figure S6. Expression levels of *AHA1* in leaves of WT, *aha2-4* and of two independent bundle-sheath-specific AHA2-complimented lines (T55, T56)

Figure S7. Knockout of AHA2 or alkaline xylem sap pH decrease $K_{leaf}$ in detached leaves.

Table S1. List of primers used for genotyping (PCR) and expression quantification (RT-PCR) of AHA1 and AHA2 in mutants and transformed plants.

## References and Notes

Alleva K, Niemietz CM, Sutka M, Maurel C, Parisi M, Tyerman SD, Amodeo G (2006) Plasma membrane of Beta vulgaris storage root shows high water channel activity regulated by cytoplasmic pH and a dual range of calcium concentrations. Journal of Experimental Botany 57: 609–621

Attia Z, Dalal A, Moshelion M (2018) Vascular bundle sheath and mesophyll regulation of leaf water balance in response to chitin. bioRxiv. doi: 10.1101/337709

Axelsen KB, Palmgren MG (2001) Inventory of the superfamily of P-type ion pumps in Arabidopsis. Plant Physiology 126: 696–706

Clough SJ, Bent AF (1998) Floral dip: A simplified method for Agrobacterium-mediated transformation of Arabidopsis thaliana. Plant Journal 16: 735–743

Fahad S, Bajwa AA, Nazir U, Anjum SA, Farooq A, Zohaib A, Sadia S, Nasim W, Adkins S, Saud S, et al (2017) Crop production under drought and heat stress: plant responses and management options. Frontiers in Plant Science 8: 1–16

Falhof J, Pedersen JT, Fuglsang AT, Palmgren M (2016) Plasma membrane H+-ATPase regulation in the center of plant physiology. Molecular Plant 9: 323–337

Frick A, Järvå M, Törnroth-Horsefield S (2013) Structural basis for pH gating of plant aquaporins. FEBS Letters 587: 989–993

bioRxiv preprint doi: https://doi.org/10.1101/234286; this version posted October 18, 2018. The copyright holder for this preprint (which was not certified by peer review) is the author/funder, who has granted bioRxiv a license to display the preprint in perpetuity. It is made available under aCC-BY-ND 4.0 International license.



Fuglsang AT, Guo Y, Cuin T a, Qiu Q, Song C, Kristiansen K a, Bych K, Schulz A, Shabala S, Schumaker KS, et al (2007) Arabidopsis protein kinase PKS5 inhibits the plasma membrane H+ -ATPase by preventing interaction with 14-3-3 protein. The Plant Cell 19: 1617–34

Geilfus CM (2017) The pH of the apoplast: dynamic factor with functional impact under stress. Molecular Plant 10: 1371–1386

Goh CH, Kinoshita T, Oku T, Shimazaki K (1996) Inhibition of blue light-dependent H+ pumping by abscisic acid in Vicia guard-cell protoplasts. Plant Physiology 111: 433–440

Grignon C, Sentenac H (1991) pH and ionic conditions in the apoplast. Annual Review of Plant Physiology and Plant Molecular Biology 42: 104–121

Hartung W, Radin JW, Hendrix DL (1988) Abscisic acid movement into the apoplastic solution of water-stressed cotton leaves: role of apoplastic pH. Plant Physiology 86: 908–913

Haruta M, Burch HL, Nelson RB, Barrett-Wilt G, Kline KG, Mohsin SB, Young JC, Otegui MS, Sussman MR (2010) Molecular characterization of mutant Arabidopsis plants with reduced plasma membrane proton pump activity. The Journal of Biological Chemistry 285: 17918–29

Hoffmann B, Kosegarten H (1995) FITC-dextran for measuring apoplast pH and apoplastic pH gradients between various cell types in sunflower leaves. Physiologia Plantarum 95: 327–335

Hoffmann B, Planker R, Mengel K (1992) Measurements of pH in the apoplast of sunflower leaves by means of fluorescence. Physiologia Plantarum 84: 146–153

Jia W, Davies WJ (2007) Modification of leaf apoplastic pH in relation to stomatal sensitivity to root-sourced abscisic acid signals. Plant Physiology 143: 68–77

Kinsman EA, Pyke KA (1998) Bundle sheath cells and cell-specific plastid development in Arabidopsis leaves. Development (Cambridge, England) 125: 1815–1822

bioRxiv preprint doi: https://doi.org/10.1101/234286; this version posted October 18, 2018. The copyright holder for this preprint (which was not certified by peer review) is the author/funder, who has granted bioRxiv a license to display the preprint in perpetuity. It is made available under aCC-BY-ND 4.0 International license.



Korovetska H, Novák O, Jůza O, Gloser V (2014) Signalling mechanisms involved in the response of two varieties of *Humulus lupulus* L. to soil drying: I. changes in xylem sap pH and the concentrations of abscisic acid and anions. Plant and Soil 380: 375–387

Lamdan NL, Attia Z, Moran N, Moshelion M (2012) The Arabidopsis-related halophyte *Thellungiella halophila*: boron tolerance via boron complexation with metabolites? Plant, Cell & Environment 35: 735–46

Leitão L, Prista C, Moura TF, Loureiro-Dias MC, Soveral G (2012) Grapevine aquaporins: Gating of a tonoplast intrinsic protein (TIP2;1) by cytosolic pH. PLoS ONE. doi: 10.1371/journal.pone.0033219

Martre P, Durand JL, Cochard H (2000) Changes in axial hydraulic conductivity along elongating leaf blades in relation to xylem maturation in tall fescue. New Phytologist 146: 235–247

Mengel K (1994) Iron availability in plant tissues-iron chlorosis on calcareous soils. Plant and Soil 165: 275–283

Moshelion M, Moran N, Chaumont F (2004) Dynamic changes in the osmotic water permeability of protoplast plasma membrane. Plant Physiology 135: 2301–2317

Mühling KH, Plieth C, Hansen U, Sattelmacher B (1995) Apoplastic pH of intact leaves of *Vicia faba* as influenced by light. Journal of Experimental Botany 46: 377–382

Palmgren MG (2001) Plant plasma membrane H+ -ATPases□: Powerhouse for nutrient uptake. Annu Rev Plant Physiol Plant Mol Biol 52: 817–45

Pantin F, Monnet F, Jannaud D, Costa JM, Renaud J, Muller B, Simonneau T, Genty B (2013) The dual effect of abscisic acid on stomata. New Phytologist 197: 65–72

Paulo J. Magalhães (2004) Ratio Plus (ImageJ) https://imagej.nih.gov/ij/plugins/ratio-plus.html.

Pitann B, Kranz T, Mühling KH (2009) The apoplastic pH and its significance in

bioRxiv preprint doi: https://doi.org/10.1101/234286; this version posted October 18, 2018. The copyright holder for this preprint (which was not certified by peer review) is the author/funder, who has granted bioRxiv a license to display the preprint in perpetuity. It is made available under aCC-BY-ND 4.0 International license.



adaptation to salinity in maize (Zea mays L.): Comparison of fluorescence microscopy and pH-sensitive microelectrodes. Plant Science 176: 497–504

Sade N, Shatil-Cohen A, Attia Z, Maurel C, Boursiac Y, Kelly G, Granot D, Yaaran A, Lerner S, Moshelion M (2014) The role of plasma membrane aquaporins in regulating the bundle sheath-mesophyll continuum and leaf hydraulics. Plant Physiology 166: 1609–20

Schroeder JI, Allen GJ, Hugouvieux V, Kwak JM, Waner D (2001) Guard cell signal transduction. Annual Review of Plant Physiology and Plant Molecular Biology 52: 627–658

Serrano R (1988) Structure and function of proton translocafing ATPase in plasma membranes of plants and fungi. Biochimica et Biophysica Acta (BBA) - Reviews on Biomembranes 947: 1–28

Shapira O, Israeli Y, Shani U, Schwartz A (2013) Salt stress aggravates boron toxicity symptoms in banana leaves by impairing guttation. Plant, Cell and Environment 36: 275–287

Shapira O, Khadka S, Israeli Y, Shani U, Schwartz A (2009) Functional anatomy controls ion distribution in banana leaves: Significance of Na + seclusion at the leaf margins. Plant, Cell and Environment 32: 476–485

Shatil-Cohen A, Attia Z, Moshelion M (2011) Bundle-sheath cell regulation of xylem-mesophyll water transport via aquaporins under drought stress: a target of xylem-borne ABA? The Plant Journal 67: 72–80

Shatil-Cohen A, Moshelion M (2012) Smart pipes: the bundle sheath role as xylem-mesophyll barrier. Plant Signaling & Behavior 7: 1088–91

Shatil-Cohen A, Sibony H, Draye X, Chaumont F, Moran N, Moshelion M (2014) Measuring the osmotic water permeability coefficient (Pf) of spherical cells: isolated plant protoplasts as an example. Journal of Visualized Experiments : JoVE e51652

Sze H, Li X, Palmgren M (1999) Energization of plant cell membranes by H+-pumping ATPases. Regulation and biosynthesis. The Plant Cell 11: 677–690

bioRxiv preprint doi: https://doi.org/10.1101/234286; this version posted October 18, 2018. The copyright holder for this preprint (which was not certified by peer review) is the author/funder, who has granted bioRxiv a license to display the preprint in perpetuity. It is made available under aCC-BY-ND 4.0 International license.



Taiz L, Zeiger E (2014) Plant Physiology and Development. doi: 10.3119/0035-4902-117.971.397

Tournaire-Roux C, Sutka M, Javot H, Gout E, Gerbeau P, Luu DT, Bligny R, Maurel C (2003) Cytosolic pH regulates root water transport during anoxic stress through gating of aquaporins. Nature 425: 393–397

Turgeman T, Shatil-Cohen A, Moshelion M, Teper-Bamnolker P, Skory CD, Lichter A, Eshel D (2016) The role of aquaporins in ph-dependent germination of Rhizopus delemar spores. PLoS ONE 11: 1–18

Wang Y, Liu F, Jensen CR (2012) Comparative effects of deficit irrigation and alternate partial root-zone irrigation on xylem pH, ABA and ionic concentrations in tomatoes. Journal of Experimental Botany 63: 1907–1917

Wigoda N, Pasmanik-Chor M, Yang T, Yu L, Moshelion M, Moran N (2017) Differential gene expression and transport functionality in the bundle sheath versus mesophyll – a potential role in leaf mineral homeostasis. Journal of Experimental Botany 68: 3179–3190

Wilkinson S, Corlett JE, Oger L, Davies WJ (1998) Effects of xylem pH on transpiration from wild-type and flacca tomato leaves1. Plant Physiology 117: 703–709

Wilkinson S, Davies WJ (1997) Xylem sap pH increase: A drought signal received at the apoplastic face of the guard cell that involves the suppression of saturable abscisic acid uptake by the epidermal symplast. Plant Physiology 113: 559–573

Wysocka-Diller JW, Helariutta Y, Fukaki H, Malamy JE, Benfey PN (2000) Molecular analysis of SCARECROW function reveals a radial patterning mechanism common to root and shoot. Development (Cambridge, England) 127: 595–603

Zhang X, Wang H, Takemiya A, Song C, Kinoshita T, Shimazaki K (2004) Inhibition of blue light-dependent H 1 Pumping by abscisic acid through hydrogen peroxide-induced dephosphorylation of the plasma membrane. Plant

bioRxiv preprint doi: https://doi.org/10.1101/234286; this version posted October 18, 2018. The copyright holder for this preprint (which was not certified by peer review) is the author/funder, who has granted bioRxiv a license to display the preprint in perpetuity. It is made available under aCC-BY-ND 4.0 International license.



Physiology 136: 4150–4158

## Main Figure Legends

**FIGURE 1. Leaf xylem sap pH reduced by petiole-fed fusicoccin (an AHA stimulator), and increased by vanadate (an AHA inhibitor)** in minor veins in detached leaves of WT (wild type) Arabidopsis. **A.** Representative images of treatment effects with color-coded pH values calculated ratiometrically for all pixels which passed the selection criteria (Supplementary Materials and methods), with black masking all other pixels. i, low-$K^+$ control (i.e., XPS, xylem perfusion solution). ii, XPS + fusicoccin (10 µM). iii, high-$K^+$ control solution (XPS +10 mM $KNO_3$). iv, XPS +10 mM $KNO_3$ + vanadate (1 mM $Na_3VO_4$). **B.** The mean (±SE) xylem sap pH without and with fusicoccin in the indicated number of leaves (biological repeats) from at least three independent experiments. Asterisks denote significant differences from the respective control, using Student's two-tailed unpaired t-test (*: $P < 0.05$, **: $P < 0.001$). Where error bar is invisible, SE= 0.009. Other details as in A. **C.** The mean (±SE) calculated values of the xylem sap pH without and with vanadate. Other details as in B.

**FIGURE 2. Knockout of *AHA2* increases xylem sap pH in minor leaf veins of Arabidopsis leaf.** *aha2* knockout lines and WT plants. The mean (±SE) xylem sap pH in the indicated number of leaves, from three independent

bioRxiv preprint doi: https://doi.org/10.1101/234286; this version posted October 18, 2018. The copyright holder for this preprint (which was not certified by peer review) is the author/funder, who has granted bioRxiv a license to display the preprint in perpetuity. It is made available under aCC-BY-ND 4.0 International license.



experiments. Different letters denote significantly different pH values ($P< 0.05$; ANOVA).

**FIGURE 3. Expression levels of *AHA2* and *AHA1* and xylem sap pH in leaves of WT, *aha2-4*, and in two independent bundle-sheath-specific AHA2-complimented lines (T55, T56)**. **A.** Mean normalized (±SE) *AHA2* expression levels obtained by qRT-PCR on whole leaf RNA (n=5 biological repetitions, leaves; see Suppl. Materials and methods). **B.** Mean (±SE) xylem sap pH in the indicated number of leaves from three independent experiments. Different letters indicate significantly different means ($P<.0.05$; ANOVA). **C.** Mean normalized (±SE) *AHA1* expression levels; other details as in A.

**FIGURE 4. The leaf hydraulic conductance ($K_{leaf}$) depends on the activity of AHA2 and the pH of the xylem perfusion solution (XPS).** Mean (±SE) $K_{leaf}$ (calculated as in Suppl. Fig. S5A) in detached Arabidopsis leaves. **A.** leaves of WT and *AHA2* knockout plants perfused with non-buffered XPS. Numbers are those of assayed leaves. Different letters indicate significantly different means ($P<.0.05$; ANOVA). Note that $K_{leaf}$ is lower in the *AHA2* knockouts relative to WT. **B.** WT Arabidopsis leaves fed with $XPS^{b}$ pH-buffered as indicated, from three independent experiments. Asterisk indicates significantly different means ($P<.0.05$; Students non-paired two-tailed t-test). Note that $K_{leaf}$ is lower at alkaline pH relative to acidic pH. A and B results are from experiments done at different time and with different solutions (see Materials and Methods).

**Figure 5: The effect of pH treatment on the membrane osmotic water permeability coefficient ($P_f$) of BSCs from SCR:GFP plants**. **A.** Time course (60 sec) of bundle sheath protoplasts swelling upon exposure to a hypotonic $XPS^{db}$ solution at pH 6 or 7.5. The arrow indicates onset of bath flush. **B.** Time course of the osmotic concentration change in the bath ($C_{out}$) during the hypotonic challenge (calculated as in Moshelion et al., 2004). **C.** Mean (±SE) initial $P_f$ values of the

bioRxiv preprint doi: https://doi.org/10.1101/234286; this version posted October 18, 2018. The copyright holder for this preprint (which was not certified by peer review) is the author/funder, who has granted bioRxiv a license to display the preprint in perpetuity. It is made available under aCC-BY-ND 4.0 International license.



indicated number of bundle sheath protoplasts under the different pHs from three independent experiments. The asterisk denotes a significant difference between the treatments using Student's two-tailed unpaired t-test ($P < 0.01$)

bioRxiv preprint doi: https://doi.org/10.1101/234286; this version posted October 18, 2018. The copyright holder for this preprint (which was not certified by peer review) is the author/funder, who has granted bioRxiv a license to display the preprint in perpetuity. It is made available under aCC-BY-ND 4.0 International license.

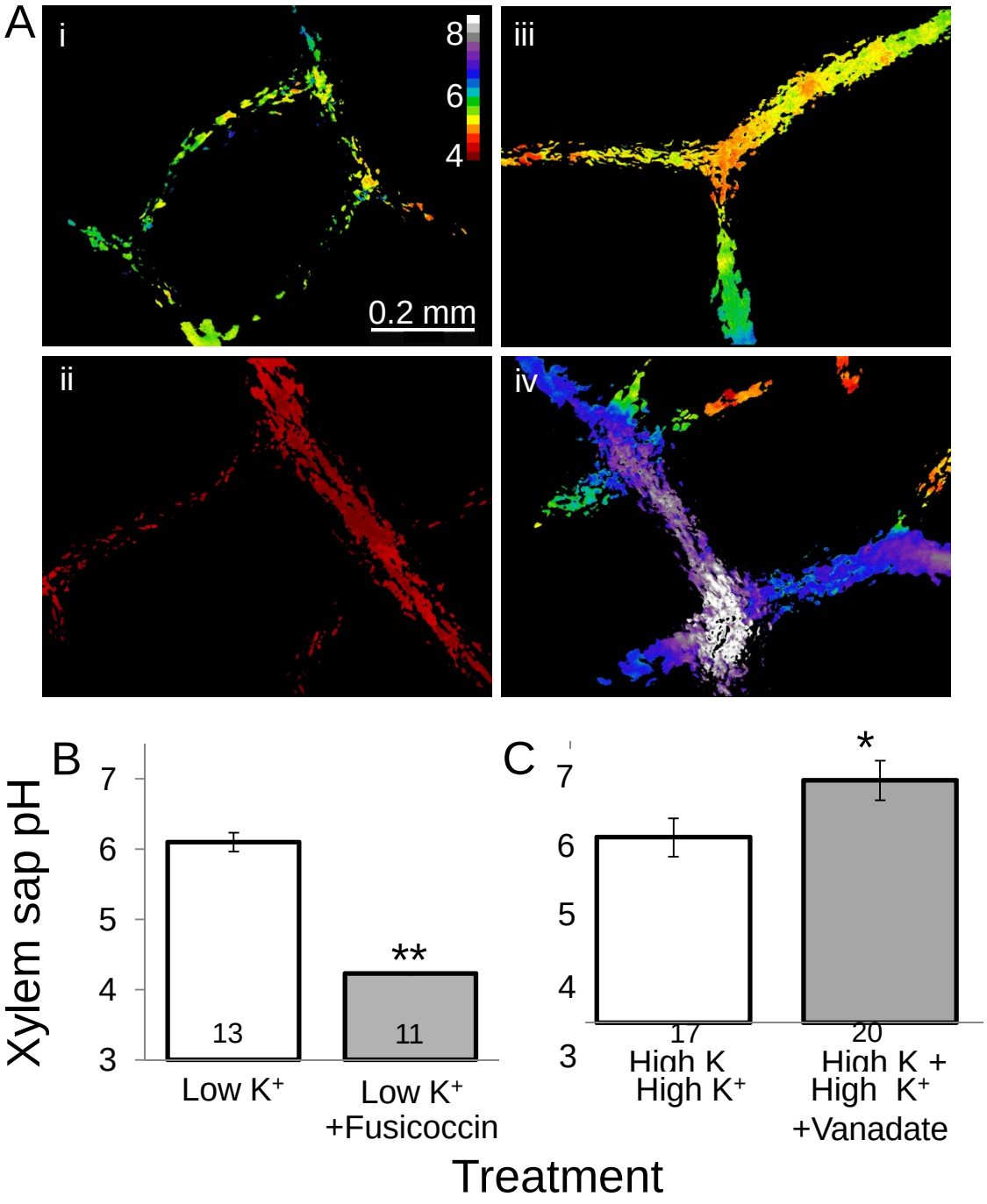


**FIGURE 1. Leaf xylem sap pH reduced by petiole-fed fusicoccin (an AHA stimulator), and increased by vanadate (an AHA inhibitor)** in minor veins in detached leaves of WT (wild type) Arabidopsis. **A.** Representative images of treatment effects with color-coded pH values calculated ratiometrically for all pixels which passed the selection criteria (Supplementary Materials and methods), with black masking all other pixels. i, low-$K^+$ control (i.e., XPS, xylem perfusion solution). ii, XPS + fusicoccin (10 μM). iii, high-$K^+$ control solution (XPS +10 mM $KNO_3$). iv, XPS +10 mM $KNO_3$ + vanadate (1 mM $Na_3VO_4$). **B.** The mean (±SE) xylem sap pH without and with fusicoccin in the indicated number of leaves (biological repeats) from at least three independent experiments. Asterisks denote significant differences from the respective control, using Student's two-tailed unpaired t-test (*: $P < 0.05$, **: $P < 0.001$). Where error bar is invisible, SE= 0.009. Other details as in A. **C.** The mean (±SE) calculated values of the xylem sap pH without and with vanadate. Other details as in B.

Fig. 1. Grunwald, Wigoda et al, 2018

bioRxiv preprint doi: https://doi.org/10.1101/234286; this version posted October 18, 2018. The copyright holder for this preprint (which was not certified by peer review) is the author/funder, who has granted bioRxiv a license to display the preprint in perpetuity. It is made available under aCC-BY-ND 4.0 International license.

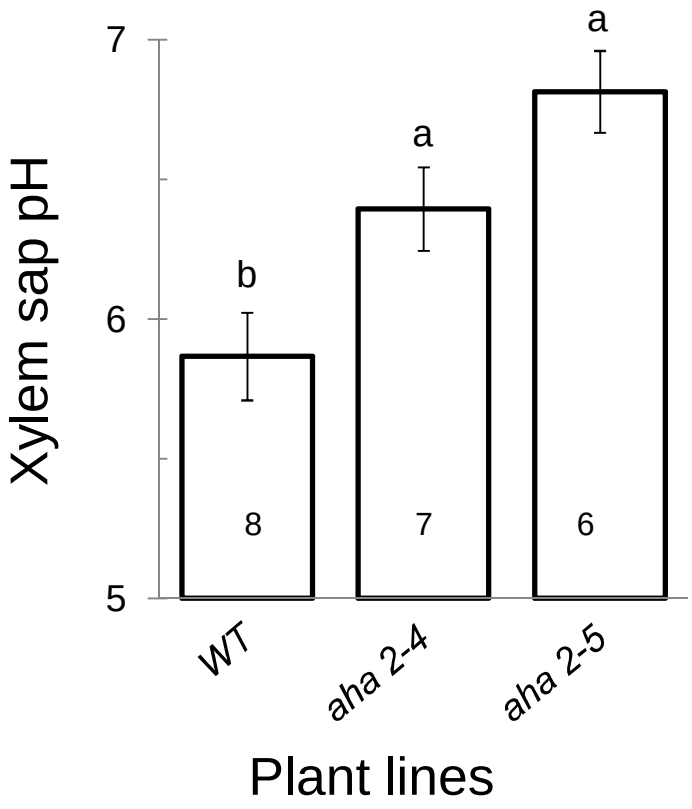


**FIGURE 2. Knockout of *AHA2* increases xylem sap pH in minor leaf veins of Arabidopsis leaf.** *aha2* knockout lines and WT plants. The mean (±SE) xylem sap pH in the indicated number of leaves, from three independent experiments. Different letters denote significantly different pH values ($P < 0.05$; ANOVA).

Fig. 2. Grunwald, Wigoda et al, 2018

bioRxiv preprint doi: https://doi.org/10.1101/234286; this version posted October 18, 2018. The copyright holder for this preprint (which was not certified by peer review) is the author/funder, who has granted bioRxiv a license to display the preprint in perpetuity. It is made available under aCC-BY-ND 4.0 International license.

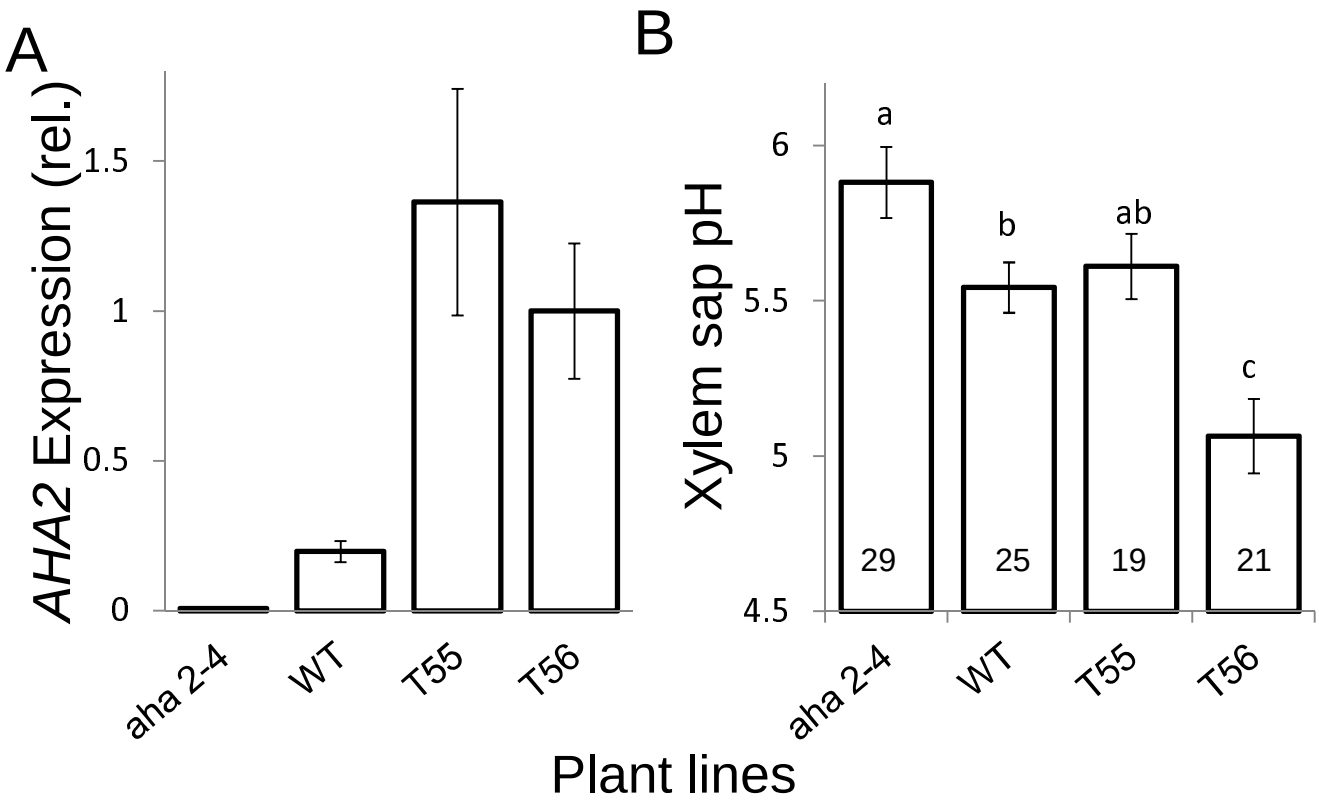


**FIGURE 3. Expression levels of *AHA2* and xylem sap pH in leaves of WT, *aha2-4* and of two independent bundle-sheath-specific AHA2-complimented lines (T55, T56)**. **A.** Mean normalized (±SE) *AHA2* expression levels obtained by qRT-PCR on whole leaf RNA (n=5 biological repetitions, leaves; see Suppl. Materials and methods). **B.** Mean (±SE) xylem sap pH in the indicated number of leaves from three independent experiments. Different letters indicate significantly different means ($P<.0.05$; ANOVA).

Fig. S6. Grunwald, Wigoda et al, 2018

bioRxiv preprint doi: https://doi.org/10.1101/234286; this version posted October 18, 2018. The copyright holder for this preprint (which was not certified by peer review) is the author/funder, who has granted bioRxiv a license to display the preprint in perpetuity. It is made available under aCC-BY-ND 4.0 International license.

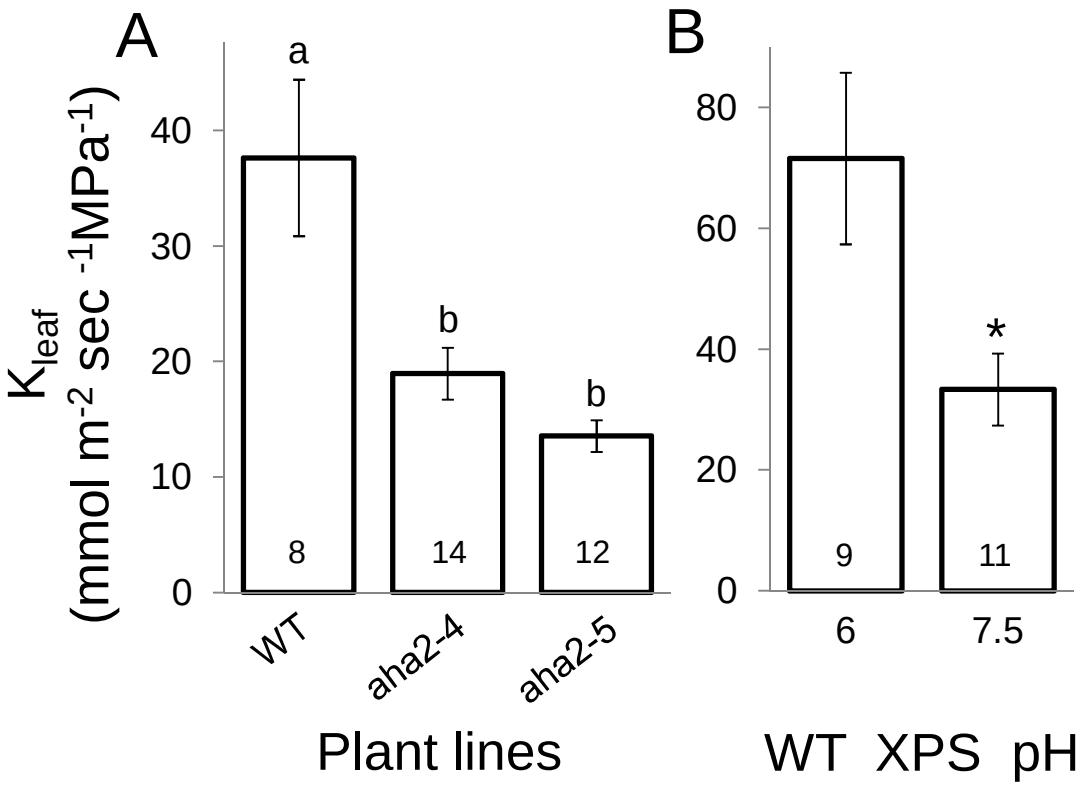


**FIGURE 4. The leaf hydraulic conductance ($K_{leaf}$) depends on the activity of AHA2 and the pH of the xylem perfusion solution (XPS).** Mean (±SE) $K_{leaf}$ (calculated by Eq. 1, Materials and Methods) in detached Arabidopsis leaves. **A.** leaves of WT and *AHA2* knockout plants perfused with non-buffered XPS. Numbers are those of assayed leaves (in three independent experiments). Different letters indicate significantly different means ($P<.0.05$; ANOVA). Note that $K_{leaf}$ is lower in the *AHA2* knockouts relative to WT. **B.** WT Arabidopsis leaves fed with $XPS^{b}$ with the indicated pH. Asterisk indicates significantly different means ($P<.0.05$; Students non-paired two-tailed t-test). Note that $K_{leaf}$ is lower at alkaline pH relative to acidic pH. Other figure details are as in A. A and B results are from experiments done at different time regimes and with different solutions (see Materials and Methods).

Fig. 4. Grunwald, Wigoda et al, 2018

bioRxiv preprint doi: https://doi.org/10.1101/234286; this version posted October 18, 2018. The copyright holder for this preprint (which was not certified by peer review) is the author/funder, who has granted bioRxiv a license to display the preprint in perpetuity. It is made available under aCC-BY-ND 4.0 International license.

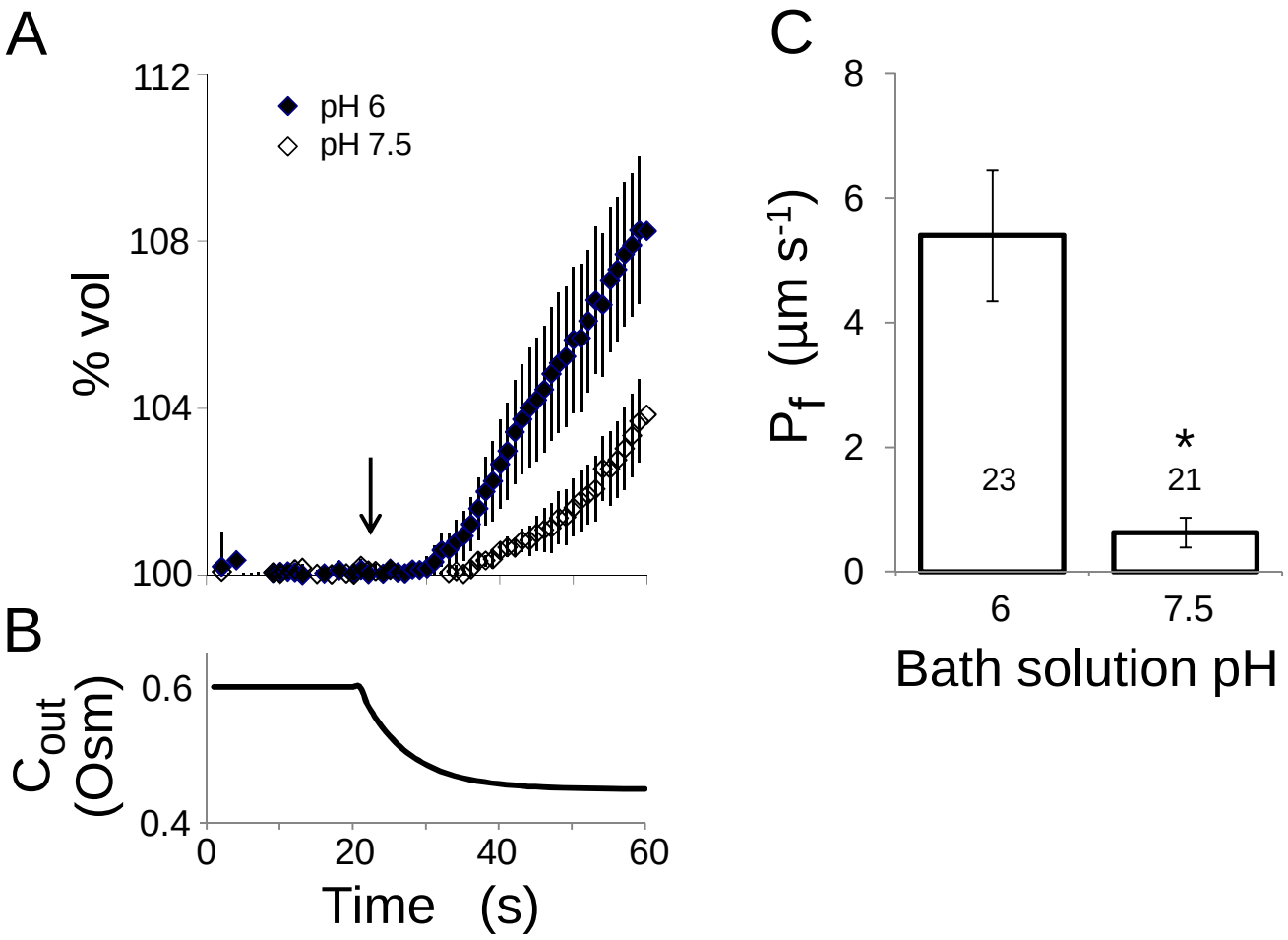


**Figure 5: The effect of pH treatment on the membrane osmotic water permeability coefficient ($P_f$) of BSCs from SCR:GFP plants**. **A.** Time course (60 sec) of bundle sheath protoplasts swelling upon exposure to a hypotonic $XPS^{db}$ solution at pH 6 or 7.5. The arrow indicates onset of bath flush. **B.** Time course of the osmotic concentration change in the bath (Cout) during the hypotonic challenge (calculated as in Moshelion et al., 2004) . **C.** Mean (±SE) initial $P_f$ values of the indicated number of bundle sheath protoplasts under the different pHs from three independent experiments. The asterisk denotes a significant difference between the treatments using Student's two-tailed unpaired t-test ($P < 0.01$).

Fig. 5. Grunwald, Wigoda et al, 2018